J. Resour. Ecol. 2017 8(6) 559-570
DOI: 10.5814/j.issn.1674-764x.2017.06.002
www.jorae.cn

Spatio-temporal Distribution of Drought in the Belt and Road Area During 1998–2015 Based on TRMM Precipitation Data

BAI Yongqing[1,2], WANG Juanle[1,3*], WANG Yujie[1,4], HAN Xuehua[1,2], Bair Z. Tsydypov[5], Altansukh Ochir[6], Davaadorj Davaasuren[7]

1. State Key Laboratory of Resources and Environmental Information System, Institute of Geographic Sciences and Natural Resources Research, Chinese Academy of Sciences, Beijing 100101, China;
2. University of Chinese Academy of Sciences, Beijing 100049, China;
3. Jiangsu Center for Collaborative Innovation in Geographical Information Resource Development and Application, Nanjing 210023, China;
4. Shandong University of Technology, Zibo, Shandong 255012, China;
5. Baikal Institute of Nature Management, Siberian Branch, Russian Academy of Sciences, Ulan-Ude 670047, Russia;
6. School of Engineering and Applied Sciences, National University of Mongolia, Ulaanbaatar city 210646, Mongolia;
7. Department of the Geography School of the Art & Sciences, National University of Mongolia, Ulaanbaatar city 210646, Mongolia

Abstract: Drought is a worldwide natural disaster that has long affected agricultural production as well as social and economic activities. Frequent droughts have been observed in the Belt and Road area, in which much of the agricultural land is concentrated in fragile ecological environment. Based on the Tropical Rainfall Measuring Mission Satellite (TRMM) 3B43 precipitation data, we used the Precipitation Abnormity Percentage drought model to study the monthly spatio-temporal distribution of drought in south region of N50° of the Belt and Road area. It was observed that drought during winter was mainly distributed in Northeast Asia, Southeast Asia, and South Asia, while it was mainly distributed in Central Asia and West Asia during summer. The occurrence of historical droughts indicates an obvious seasonal cycle. The regional variations in drought were analyzed using the Breaks for Additive Season and Trend tool (BFAST) in six sub-regions according to the spatial distribution of six economic corridors in the Belt and Road area. The average drought conditions over the 18 years show a slight decreasing trend in Northeast Asia, West Asia, North Africa, South Asia, Central and Eastern Europe, and a slight increasing trend in Central Asia. However, it was a fluctuating pattern of first increasing and then decreasing in Southeast Asia. The results indicate that the total drought area in the Belt and Road region showed a general decreasing trend at a rate of 40,260 km2 per year from 1998 to 2015.

Key words: drought distribution; the Belt and Road; TRMM; Precipitation Abnormity Percentage; BFAST

1 Introduction

Drought refers to a shortage of precipitation or a circumstance in which the water supply does not meet the water requirements (Ren, 1991; Zhang, 1993; Liu *et al*., 2004). Due to their high frequencies, long duration, wide range of impacts, and a large number of accompanying disasters, droughts have been known to cause great economic losses to the national economies, especially to agricultural production, in many countries (Ye, 1996; Wilhite, 2000; Han *et al*., 2014; Sun *et al*., 2014). The United Nations report in March 2015 showed that the worldwide annual economic losses caused by natural disasters, such as earthquakes, floods, droughts, and tornadoes, have reached an average of

Received: 2017-04-22 **Accepted:** 2017-08-02
Foundation: Construction Project of China Knowledge Center for Engineering Sciences and Technology (CKCEST-2017-3-1); Cultivate Project of Institute of Geographic Sciences and Natural Resources Research, Chinese Academy of Science (TSYJS03); National University of Mongolia (P2017-2396)
***Corresponding author:** WANG Juanle, E-mail: wangjl@igsnrr.ac.cn

Citation: BAI Yongqing, WANG Juanle, WANG Yujie, *et al*. 2017. Spatio-temporal Distribution of Drought in the Belt and Road Area during 1998–2015 Based on TRMM Precipitation Data. *Journal of Resources and Ecology*, 8(6): 559–570.

$250–300 billion (China News Service, 2015). In February, 2016, the Belgian Center for Disaster Epidemiology Research (CRED) issued a bulletin entitled "Disaster data for 2015" jointly with the United Nations International Strategy for Disaster Reduction (UNISDR) and the United States Agency for International Development (USAID). The report pointed out that in 2015 meteorological disasters were the main global natural disaster. Additionally, thirty-two major droughts were recorded through the year, a number twice the annual average of the past decade. The number of people affected by drought was 50.5 million, much higher than the average of 35.4 million over the past 10 years (UNISDR and CRED, 2016; Pei, 2016).

In 2013, Chinese President Xi Jinping proposed the construction of the Silk Road Economic Belt and the 21st century Maritime Silk Road (hereinafter referred to as the Belt and Road) Initiative aimed at creating an open, inclusive, balanced, and advantageous regional economic cooperation framework among the countries in the area (National Development and Reform Commission, 2015). There is a large population in the Belt and Road area with diverse cultures and an extremely uneven economic development. Under the dual impacts of natural and human activities, the Belt and Road areas are facing a series of major long-term problems including global changes, ecological deterioration, resource crises, and poverty. Frequent meteorological disasters, especially droughts, have serious impacts on agricultural production in various countries. The countries along the area have invested relatively less in disaster prevention, disaster reduction, and disaster relief due to the limitations of economic development which would lead to very serious losses in the event of a disaster. Accurate understanding of the severity of historical drought cases, variation in patterns of drought, and the underlying relationship between drought and the geographical environment can support the decision-making process regarding the response and alleviation of drought losses in the region as well as the implementation of global disaster prevention and mitigation projects.

Methods of meteorology are typically used in drought monitoring to study the statistical distribution of precipitation to determine the intensity and duration of droughts (Li *et al*., 2010). In recent years, satellite remote sensing technology has been developed vigorously as an essential method for ground monitoring and information acquisition because of its short observation period, ease of availability, and wide spatial range, which could achieve rapid quantitative analysis and reduce field work to improve work efficiency (Liu *et al*., 2012). As early as the 1960s, there was a study on the characterization of drought by monitoring soil moisture using remote sensing (Bartholic *et al*., 1962; Curran, 1979). In the late 1980s, droughts occurred in large parts of the United States (US) and seriously affected crop growth. The US scientists used NOAA/AVHRR satellite images to extract vegetation indices to monitor and assess the drought condition which supported the government decisions (Huete, 1988). Since the 1990s, meteorological satellite remote sensing technology has attracted more and more attention and thermal inertia, crop water deficit index, surface temperature, and vegetation indexes have been used coherently in drought monitoring researches (Liu *et al*., 2012). Rouse (1974) used the Normalized Difference Vegetation Index to monitor seasonal vegetation droughts in the central American prairie region, and Qi (2005) established the Temperature Vegetation Drought Index and the Differential Temperature Vegetation Drought Index based on MODIS data to characterize the drought severity.

Traditional drought monitoring based on meteorological station data is usually carried out for smaller areas. The number and distribution of meteorological weather stations affects the accuracy of regional monitoring results directly due to the uneven spatio-temporal distribution of regional precipitation. On the contrary, satellite remote sensing has large spatial coverage and could continuously observe the spatial distribution of global precipitation for longer periods. Considering the urgent demand for the spatio-temporal distribution of drought disasters over long periods of time in the Belt and Road region, this study utilized the Tropical Rainfall Measuring Mission satellite (TRMM) precipitation data to calculate the monthly spatio-temporal distribution of drought in the Belt and Road area from 1998 to 2015 based on the Precipitation Abnormity Percentage drought model. The changes in the patterns of drought areas in the six regions in the Belt and Road area were analyzed based on the Breaks for Additive Season and Trend (BFAST) tool. We expect to provide the results of drought remote sensing monitoring and methods for drought disaster prevention and reduction as well as for agricultural development in the region.

2 Materials and methods

2.1 Study area

Based on relevant literature regarding the countries participating in the Belt and Road initiative (Wang, 2015; Big Data Center for the Belt and Road Initiative in National Information Center, 2016; Xiao, 2016) and the sensor collection range from the TRMM precipitation remote sensing data, we selected 61 countries along the Belt and Road area, south of N50°, for our study. As shown in Fig. 1, the 61 countries lay across Asia, Europe, and Africa, with a total land area of 62.3776 million km^2. Only parts of Mongolia, Russia, China, Poland, Czech Republic, Ukraine, and Kazakhstan were included in the study.

2.2 Data

In this study, the TRMM 3B43 data were used to study the spatio-temporal distribution of meteorological drought caused by lack of precipitation. The TRMM satellite, jointly developed by the US and Japan, is the first meteorological satellite dedicated to the quantitative measurement of rainfall in tropical and subtropical regions. Its main purpose is

to further our understanding of global circulations of energy and water by studying precipitation and latent heat in the tropics. The main sensors on the satellite equipped for precipitation observation are: Precipitation Radar (PR), TRMM Microwave Imager, and Visible/Infrared Sensor. PR is the first space-borne precipitation radar and it can observe the three-dimensional structure of rainfall (Chen *et al*., 2005). The TRMM 3B43 data used in this study were obtained from the website of Goddard Earth Sciences Data and Information Services Center (http://mirador.gsfc.nasa. gov/). The dataset ranges from January, 1998 to December, 2015 in HDF format with a spatial resolution of 0.25° × 0.25°. There are 1440 × 400 grids globally and the corresponding precipitation value of the grid is the average within the grid with the units of mm/h. The monthly spatio- temporal distribution of precipitation can be summarized after some correction processing of rotation, georeferencing, and resampling.

2.3 Methods

2.3.1 Precipitation abnormity percentage

In this paper, the spatio-temporal distribution of drought in the study area was calculated using the Precipitation Abnormity Percentage drought model. The Precipitation Abnormity Percentage (P_a) is one indicator used to measure variations of precipitation compared to the normal value in a certain period. It is defined as the ratio of the difference between the actual precipitation and historical average precipitation to the historical average precipitation. It can directly reflect the drought caused by abnormal precipitation and it is suitable for periods when the average temperature is above 10°C in semi-humid, semi-arid areas (China Meteorological Administration, 2006). Table 1 shows the categories of drought levels based on the Precipitation Abnormity Percentage. In this paper, descriptions, such as extremely dry, severely dry, moderately dry, mildly dry, and no drought, are based on the standards given in the following drought classification table of Precipitation Abnormity Percentage.

The calculation method of the Precipitation Abnormity Percentage during a certain period is described by equation (1):

$$P_a = \frac{P - \overline{P}}{\overline{P}} \times 100\% \quad (1)$$

Where P is the precipitation within a certain period (mm), and $\overline{P}$ is the average precipitation within the same calculation period (mm), the calculation method is shown in equation (2):

$$\overline{P} = \frac{1}{n}\sum_{i=1}^{n} P_i \quad (2)$$

Where P is the number of months for which the average precipitation has to be determined, $i = 1, 2 \cdots n$.

2.3.2 Breaks for additive season and trend

BFAST tool decomposes the original time series data into three components, namely seasonal variations, segmented

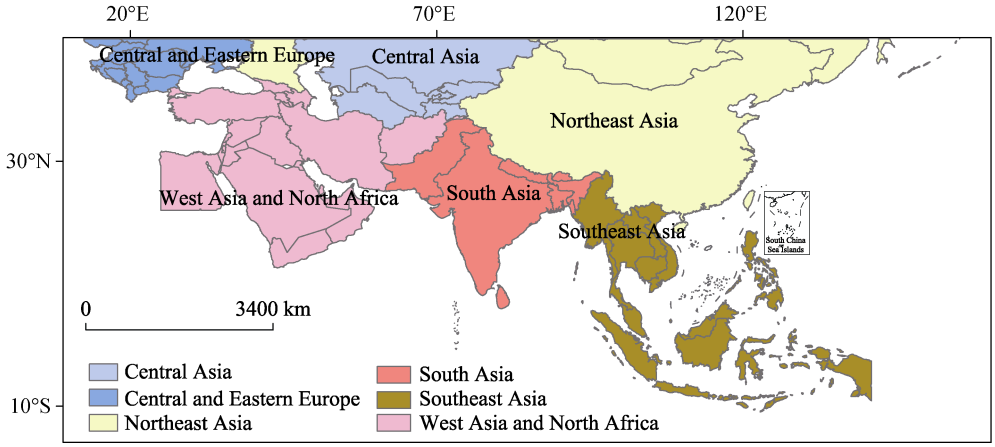

Fig.1 Research area

Table 1 Drought classification table of Precipitation Abnormity Percentage

Rank	Category	Precipitation Abnormity Percentage (%)		
		Monthly scale	Quarterly scale	Annual scale
1	No drought	$-40 < P_a$	$-25 < P_a$	$-15 < P_a$
2	Mildly dry	$-60 < P_a \leqslant -40$	$-50 < P_a \leqslant -25$	$-30 < P_a \leqslant -15$
3	Moderately dry	$-80 < P_a \leqslant -60$	$-70 < P_a \leqslant -50$	$-40 < P_a \leqslant -30$
4	Severely dry	$-95 < P_a \leqslant -80$	$-80 < P_a \leqslant -70$	$-45 < P_a \leqslant -40$
5	Extremely dry	$P_a \leqslant -95$	$P_a \leqslant -80$	$P_a \leqslant -45$

linear trends, and residuals to monitor the patterns of data variations in segments (shown in Equation (3)). The tool is widely used for monitoring long-term trends in temporal data series and inflection points, and the linear and periodic models of data variations in different segments are presented visually along with the confidence interval and the position of inflection points (Verbesselt, 2010; Verbesselt *et al*., 2012; Che *et al*., 2017). The trend component generally describes the gradual variation patterns of the time series data for more than one year during which there may be some inflection points. The seasonal component is generally expressed as a periodic change at an annual time scale. The residual component is a measure of the random variables caused by the observation methodologies, such as the signal-to-noise-ratio, and the atmospheric environment, such as clouds and aerosols (Quan *et al*., 2016). BFAST can be used to analyze various satellite temporal data series and seek seasonal or non-seasonal variation patterns. It is widely used in scientific hydrology, climatology, and econometrics researches. In this study, we used the BFAST package in the R to analyze the variation trend of the monthly average Precipitation Abnormity Percentage.

$$Y_t = T_t + S_t + e_t \ (t = 1, 2, \cdots, n) \quad (3)$$

Where Y_t denotes the observation data under time series t, T_t denotes the trend component, S_t denotes the seasonal component, and e_t denotes the residual component, which is the remaining part of the time series data except the seasonal component and the trend component.

3 Results

3.1 Validity test of tropical rainfall measuring mission satellite precipitation data

The accuracy and validity of remote sensing data is a fundamental guarantee for application analysis (Ma, 2006). The observation data of meteorological stations obtained from the China Meteorological Data Sharing Network were used as the real value to test the validity of the TRMM 3B43 precipitation data. The monthly precipitation values observed by the meteorological stations were taken as the independent variable and the average monthly precipitation values of the TRMM in the corresponding grids were taken as the dependent variable. The two groups of precipitation values were analyzed using linear regression analysis in SPSS to obtain the regression determination coefficient R^2 and the probability values between the meteorological station monitoring data and the remote sensing data.

Considering the limited time ranges of the observed meteorological station data, the validity of the precipitation data of TRMM 3B43 was tested by meteorological station data of mainland China for July from 1998 to 2013. Scatter plots and linear regression equations for the TRMM data validity analysis for July from 1998 to 2013 are shown in Fig. 2.

The validation results of the precipitation data from TRMM 3B43 for July from 1998 to 2013 (Table 2) showed that the regression analysis significance indicator R^2 ranges from 0.6389 to 0.8106. Because of the differences between the spatial scales of the two kinds of rainfall data, the monthly precipitation from TRMM is slightly different from that of the meteorological station and, overall, the precipitation observed by TRMM is slightly lower than that measured by the meteorological weather stations. Over 87 percent of the TRMM data fit well with the meteorological station data with R^2 value above 0.7. Overall, there is a clear linear correlation between the two datasets and the consistency of the two kinds of precipitation values is relatively high, making it suitable for calculation of the spatio-temporal distribution of drought in the Belt and Road area.

3.2 Distribution and variation of drought in the Belt and Road area

The distribution of monthly Precipitation Abnormity Percentages in the Belt and Road area from 1998 to 2015 was calculated according to the method for calculating the Precipitation Abnormity Percentage given in section 2.3.1. The results were reclassified according to the drought classification criteria at the monthly scale given in Table 1. Subsequently, we got the spatio-temporal distribution of drought in the study area. Fig. 3, for example, shows the spatio-temporal distribution of drought in the Belt and Road area from January to December in 1998.

According to the monthly spatio-temporal distribution of drought in the Belt and Road area during 1998–2015, there were significantly more arid regions in winter than in summer and large areas of extreme drought and severe drought occurred in Northeast Asia, Southeast Asia, South Asia, Central Asia, and West Asia. In Northeast Asia, areas of northeast China, northern China, and the southwest and central parts of Mongolia suffered the most severe drought followed by the northwest region of China. However, the southeastern coastal areas experienced relatively light drought. In Southeast Asia, the most severe drought mainly occurred in Myanmar, Laos, Thailand, and Cambodia. In South Asia, the most serious drought took place in India, Pakistan, Nepal, Bhutan, and Bangladesh. In Central Asia, the severely dry areas in Uzbekistan and Turkmenistan were the largest. In West Asia, large areas of severe drought arose in Saudi Arabia, Oman, and southern Egypt. Due to low precipitation, decrease of river flow in winter, and the monsoon climate caused by the Siberian cold, severe drought usually occurs in large areas of Southeast and South Asia in winter. In the summer, the drought area became relatively smaller and the severe drought was mainly concentrated in Central Asia and West Asia, especially in Uzbekistan, Turkmenistan, Afghanistan, Saudi Arabia, Egypt, Syria, Lebanon, Jordan, Israel, Iraq, Iran, Kuwait, Bahrain, and Qatar. From the perspective of meteorology, it is known that

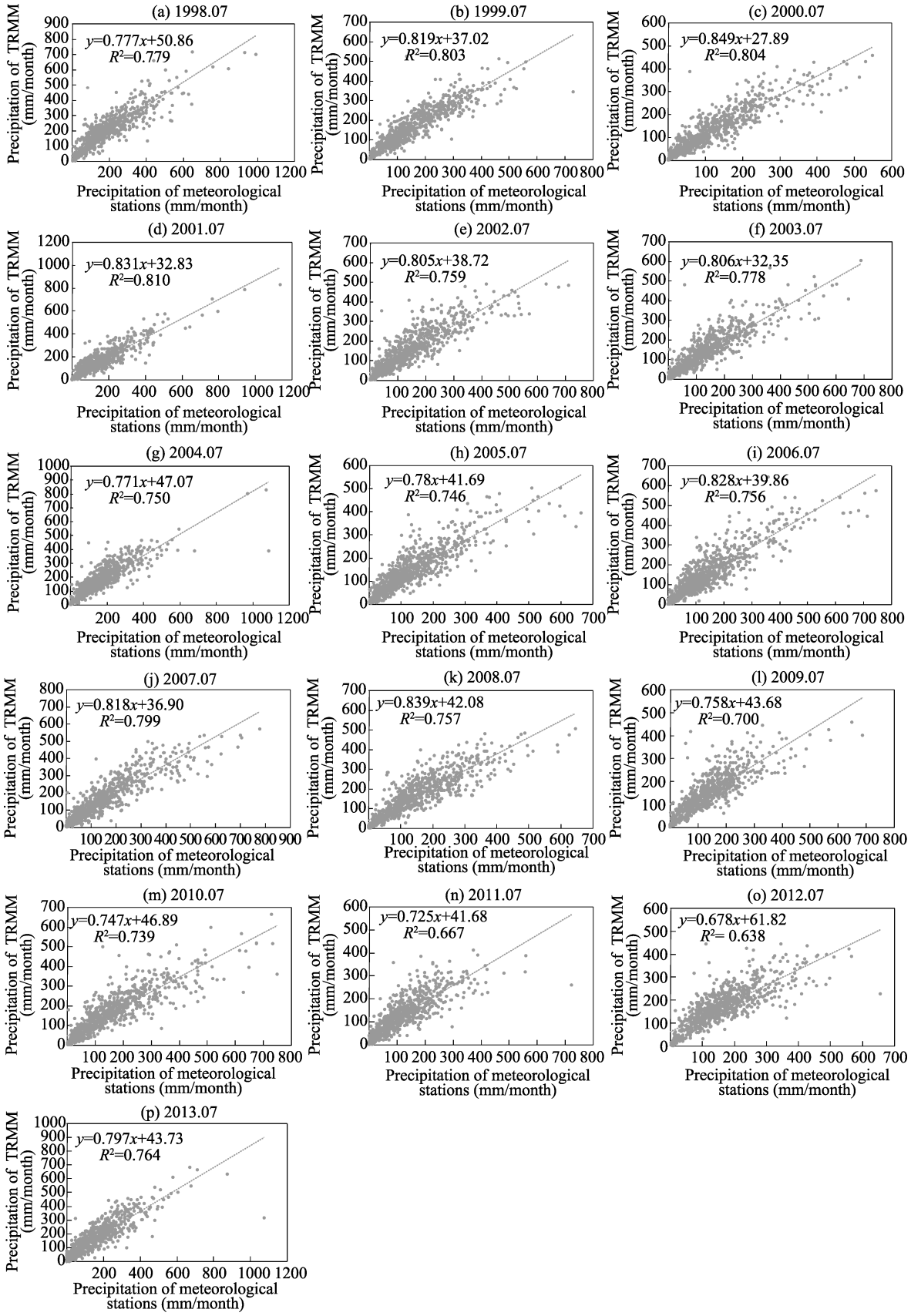

Fig.2 Scatter plots and linear regression equations of the TRMM data validity analysis

the ecological environment is fragile near the Caspian Sea, the amount of water vapor is relatively small, and the rivers are mostly inland relying on the iceberg-melt water and that the high pressure of the summer Azores leads to low precipitation and high evaporation in the East Coast area. The Red Sea area and the Persian Gulf region are usually controlled by the subtropical high pressure or the low latitude wind, therefore, subsidence airflow usually prevails, leading to scarce precipitation and a mostly tropical desert climate—hot and dry throughout the year.

By summarizing the drought conditions based on the spatio-temporal distribution of droughts in the Belt and Road area, we obtained the monthly changes of the total area of the four types of droughts (extremely dry, severely dry, moderately dry, and mildly dry) in the study area during 1998–2015. As shown in Fig. 4, the drought area in the study area reached a maximum of 23.5229 million km^2 in December, 1999 (24th month), and the minimum value of the drought area in the study area was 7.8867 million km^2 in May, 2010 (149th month). By calculating the difference in drought areas in any adjacent two months, it was observed that the drought area increased by 7.2535 million km^2 in the period between October and November, 2008 (130th–131st months), which was the maximum increase of drought area

Table 2 Validation results of TRMM precipitation data for July from 1998 to 2013

Year	Number of meteorological stations	Slope	R^2
1998	780	0.7778	0.7796
1999	781	0.8195	0.8031
2000	780	0.8498	0.8041
2001	781	0.8318	0.8106
2002	781	0.8052	0.7596
2003	783	0.8064	0.778
2004	782	0.7718	0.7503
2005	785	0.78	0.7466
2006	785	0.8287	0.756
2007	785	0.8182	0.7996
2008	786	0.8391	0.757
2009	786	0.7588	0.7008
2010	786	0.7477	0.7397
2011	785	0.7251	0.6679
2012	785	0.6782	0.6389
2013	785	0.7971	0.7642

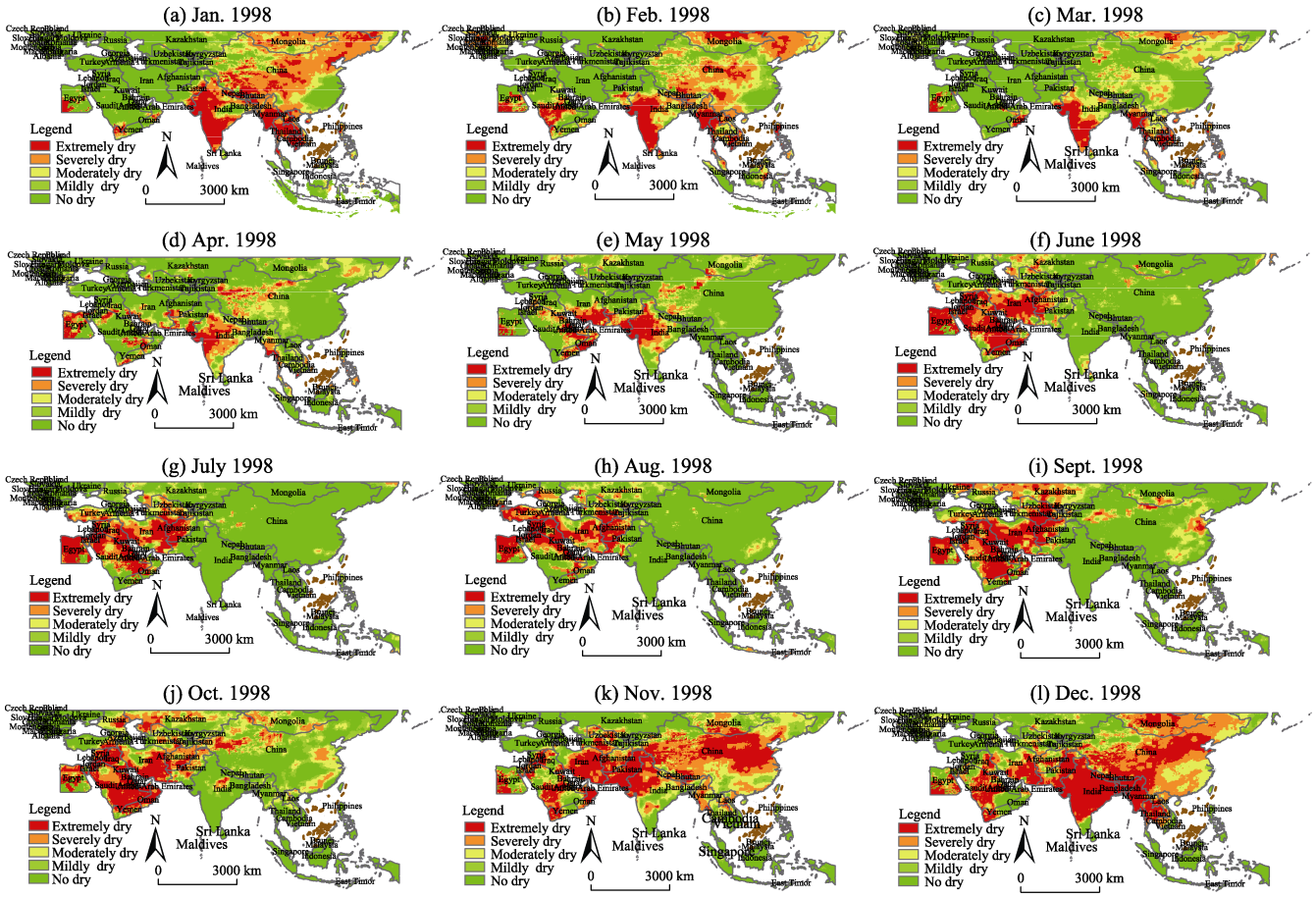

Fig.3 Spatio-temporal distribution of drought in Belt and Road area from January to December, 1998

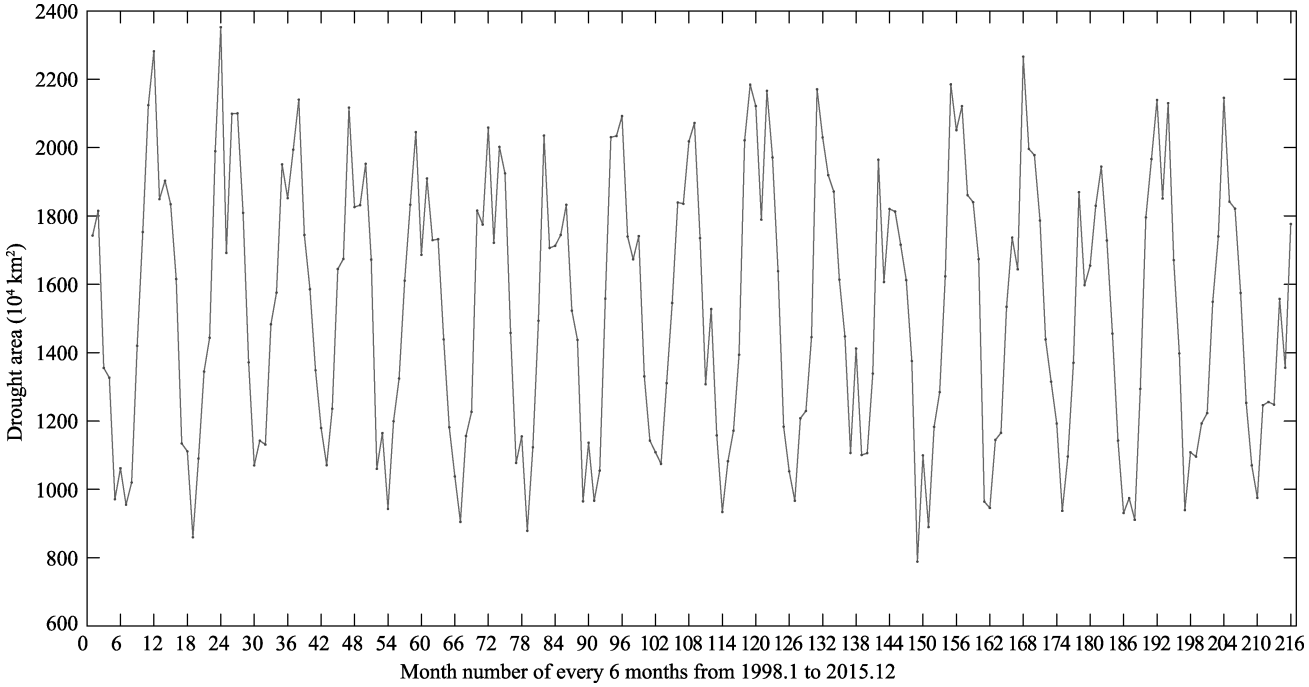

Fig.4 Monthly drought area of the Belt and Road area

over 18 years. On the contrary, the drought area reduced by 7.0907 million km^2 from April to May, 2011 (160th–161st months), which was the largest decrease in 18 years. Fig. 5 shows the trend of drought area in which the variation of drought area had obvious seasonal periodicity. The total drought area in the Belt and Road area during the 18 years shows decreasing trend at an annual rate of 40 260 km^2.

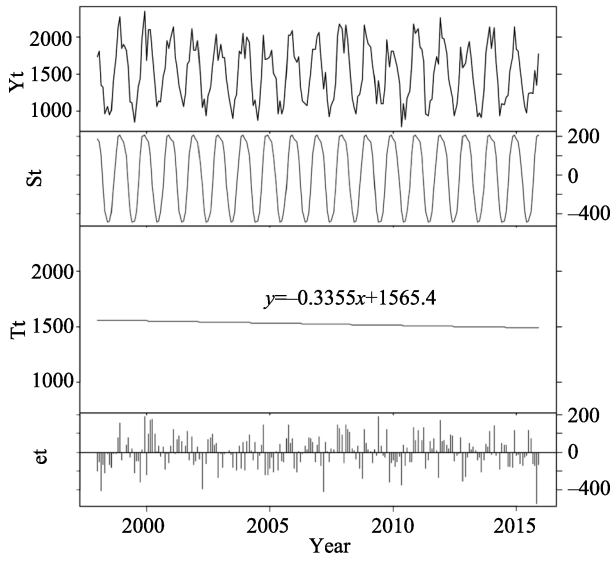

Fig.5 Trend of monthly drought area in the Belt and Road area (10^4 km^2)

Yt represents raw time series data of monthly drought area in the Belt and Road area from January, 1998 to December, 2015, St represents seasonal changes of the drought areas, Tt represents overall variation trends of the drought areas, *et* = *Yt* – *St* – *Tt*, represents residual errors of the data

4 Discussion

4.1 Regional variation patterns of drought levels

The Belt and Road area can be divided into six major economic corridors: China-Mongolia-Russia, New Asia-Europe land bridge, China-Central Asia-West Asia, China-Indo China Peninsula, China-Pakistan, and Bangladesh-China-India-Burma. Based on the spatial distribution of these six economic corridors, regional differences of drought variations were studied in the sub-regions of Northeast Asia, Southeast Asia, South Asia, West Asia, and North Africa, Central and Eastern Europe, and Central Asia.

Drought in Northeast Asia mainly occurred from November to March, and the drought conditions, characterized by the average of Precipitation Abnormity Percentages, fall within the level of moderate drought and below. Only in February, 1999 did the drought conditions reach above severe drought. There were 50 months with the drought conditions in the moderate drought level. The droughts in December, 1999 and December, 2003 became very close to severe droughts but were relatively mild in other months, and the amplitude of the variation of Precipitation Abnormity Percentage in the Northeast Asia region was –0.81–2.37. It is evident from Fig. 6a that the variation of the average drought condition in northeast Asia is very stable over 18 years, showing a slight decreasing trend, and the rate of increase of the Precipitation Abnormity Percentage is 0.012/10 yr.

The drought condition in the Southeast Asia region was less severe and the drought mostly occurred in the winter. The drought condition classified based on the monthly mean

value of the Precipitation Abnormity Percentages was mostly mildly drought. Only in February, 2014 the drought reached the level of moderately dry. There were 16 mildly dry months, in which the drought condition in February, 2014 and March, 2015 were at the brink of mild drought and no drought; the other months were at the level of no drought. Overall, Southeast Asia indicated a more humid environment compared to Northeast Asia and the variation amplitude of the Precipitation Abnormity Percentages in Southeast Asia ranged from −0.62 to 0.72. It can be seen from Fig. 6b that the average drought level in Southeast Asia from January, 1998 to August, 2002 has a decreasing trend with the Precipitation Abnormity Percentage having an increment rate of 1.5/10yr. From September, 2002 to December, 2015, the average drought level in Southeast Asia became increasing severe; however, there were two breakpoints in June, 2005 and June, 2010. The decreasing rates of Precipitation Abnormity Percentages during the three time periods were 0.384/10yr, 0.24/10yr, and 0.552/10yr, respectively.

The drought in South Asia was severe and mostly came about in the winter, and the drought conditions as evaluated by the monthly mean values of the Precipitation Abnormity Percentages, were severely dry and moderately dry. In December, 1999, the drought condition reached extremely dry. There were 30 months with the drought conditions reached the severe drought level and 38 months at the moderate drought level, in which the drought levels in January, 2002 and January, 2013 were close to severe drought. There were 43 months at mildly dry and the other months experienced no drought. The amplitude of the variations of Precipitation Abnormity Percentage in South Asia was –0.95–2.96. It can be inferred from Fig. 6c that the change of the average drought level in South Asia is relatively stable over 18 years and the overall level shows a decreasing trend in a small range. Additionally, the Precipitation Abnormity Percentage has a slight increasing trend of 0.036/10yr.

The drought in West Asia and North Africa was quite severe and occurred during the summer and autumn. The drought conditions classified by the monthly mean value of the Precipitation Abnormity Percentage were mostly in the moderate dry and mildly dry levels. In June, 1999, June, 2000 and July, June and September, 2001, June, 2002, June, 2003, June, 2004, September, 2005, June, 2006, September, 2007, July, 2008, September, 2010, and September, 2013, the drought condition for a total of 14 months was severely dry. Fifty months of drought were in the moderately dry level. Twenty-two months of drought were at the level of mild drought and the other months experienced no drought. The amplitude of the variation of the Precipitation Abnormity Percentage in West Asia and North Africa was –0.9–2.92. It can be observed from Fig. 6d that the change in the average drought level in West Asia and North Africa over 18 years is relatively stable, showing a decreasing trend over a small range and the rate of increase of the Precipitation Abnormity Percentage was 0.072/10yr.

The average drought condition in Central and Eastern Europe was mild and mostly distributed during the spring and winter and the drought conditions as classified by the monthly average of the Precipitation Abnormity Percentages were mostly in the mildly dry level. The drought level in November, 2011 reached severely dry. In October, 2000, October, 2001, March, 2003, April, 2007, February, 2008, April, 2009, September, 2011, March, 2012, December, 2013, and December, 2015, for a total of 10 months, the drought conditions reached moderately dry. There were 18 months at the mildly dry level and the other months experienced no drought. The amplitude of the variation of the Precipitation Abnormity Percentage in the Central and Eastern Europe was –0.9–0.83. It can be seen from Fig. 6e that the average drought level in Central and Eastern Europe was stable over 18 years and the overall trend was decreasing over a small range and the percentage of precipitation abnormity increased at the rate of 0.024/10yr.

The drought in the Central Asia region was mild and occurred mainly during autumn and the drought conditions as classified by the monthly mean value of the Precipitation Abnormity Percentage were mostly moderately dry and mildly dry. In September, 2005 and August, 2006, the drought condition reached severely dry. Below the severely dry level, there were 24 months in total that had a moderately dry condition. In August, 2002 (the 57th month), September, 2004, August, 2007, and August, 2008, the drought level was close to severely dry. A total of 31 months of drought were at the mildly dry level and the other months experienced no drought. The amplitude of variation of the Precipitation Abnormity Percentage in Central Asia was –0.89 –1.68. It can be seen from Fig. 6f that the average drought level in Central Asia was stable over 18 years with an overall small increase in a small range; the rate of reduction of the Precipitation Abnormity Percentage was 0.036/10yr.

It can be inferred Fig. 6 that the drought in the six sub-regions showed an obvious seasonal period. By comparing the amplitude of Precipitation Abnormity Percentages, the drought in South Asia was found to be the highest (the Precipitation Abnormity Percentage was –0.95), and the seriousness of the drought in Southeast Asia was the lowest (Precipitation Abnormity Percentage was –0.62).

4.2 Regional variation patterns of drought areas

Figure 7 shows the variation trends of drought areas of the six sub-regions of the Belt and Road area. It is observed that the drought areas of Northeast Asia (Fig. 7a), South Asia (Fig. 7c), West Asia and North Africa (Fig. 7d) represents a decreasing trend at the rates of 220.820 thousand km^2/10yr, 76.448 thousand km^2/10yr, and 241.28 thousand km^2/10yr, respectively. The drought areas of Central and Eastern Europe (Fig. 7e) and Central Asia (Fig. 7f) showed increasing trends at the rates of 14.76 thousand km^2/10yr and 58.08

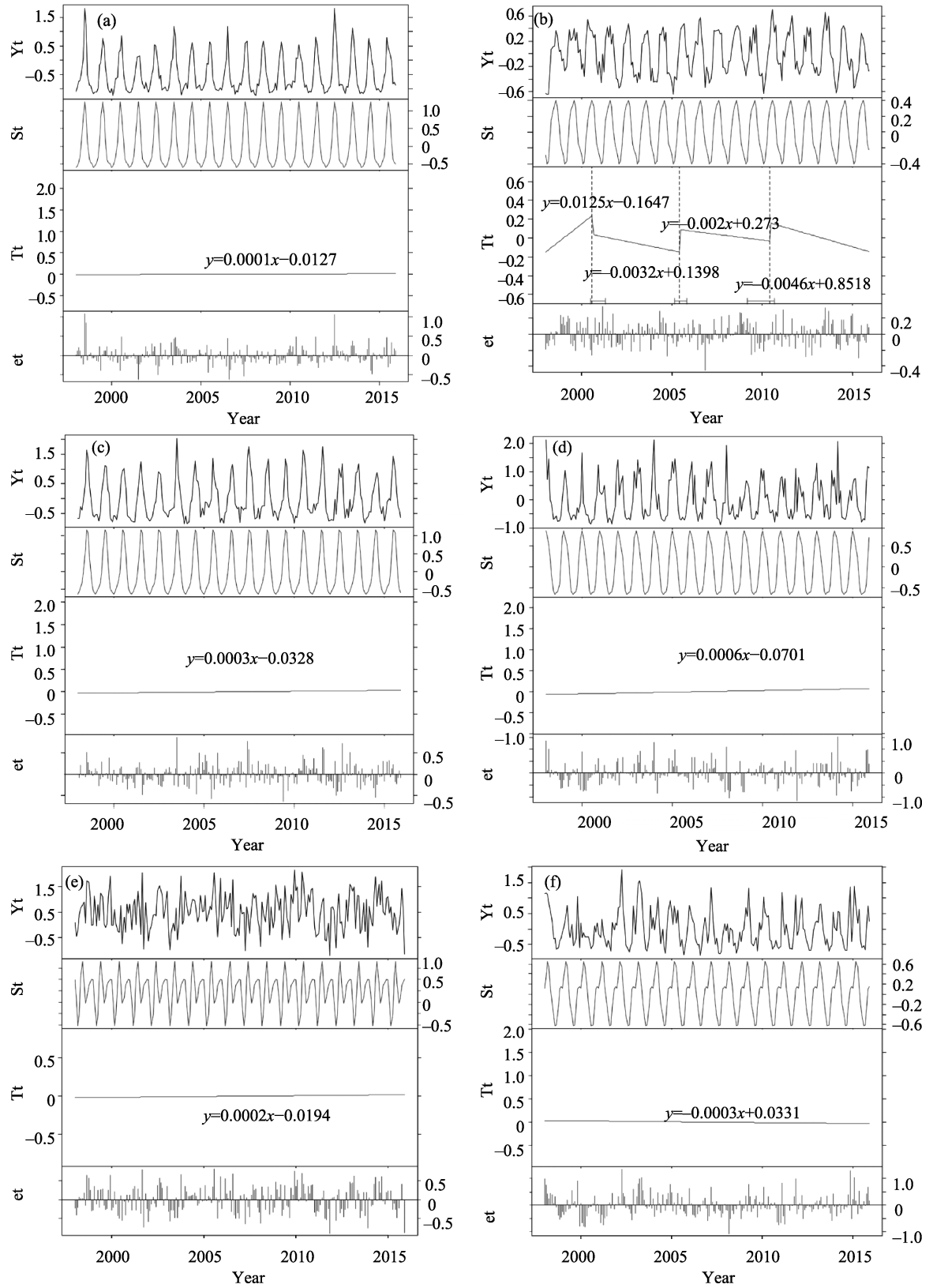

Fig.6 Trends of monthly Precipitation Abnormity Percentage for the sub-regions

(a) Northeast Asia; (b) Southeast Asia; (c) South Asia; (d) West Asia and North Africa; (e) Central and Eastern Europe; (f) Central Asia. (Yt represents raw time series data of monthly Precipitation Abnormity Percentage in the sub-regions from January, 1998 to December, 2015, St represents seasonal changes of the drought areas, Tt represents overall variation trend of the drought areas, et = Yt – St – Tt, represents residual errors of the data.)

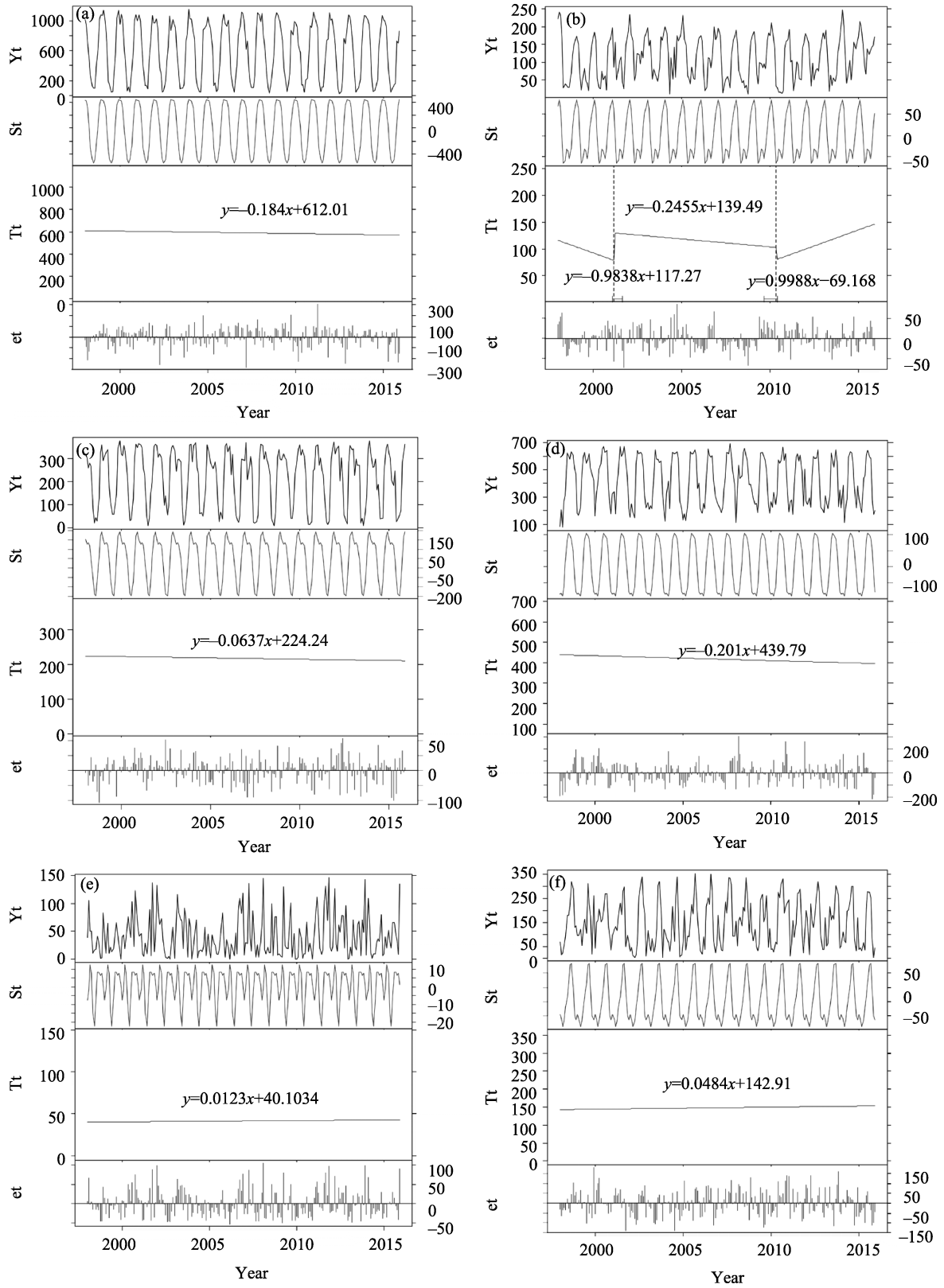

Fig.7 Trends of monthly drought areas of the sub-regions in the Belt and Road area (10^4 km^2)

(a) Northeast Asia; (b) Southeast Asia; (c) South Asia; (d) West Asia and North Africa; (e) Central and Eastern Europe; (f) Central Asia. (Yt represents raw time series data of monthly drought area in the sub-regions from January, 1998 to December, 2015, St represents seasonal changes of the drought areas, Tt represents overall variation trends of the drought areas, et = Yt – St – Tt, represents residual errors of the data.)

thousand km^2/10yr, respectively. The drought area of the Southeast Asia region (Fig. 7b) shows a decreasing trend firstly from January, 1998 to May, 2010, with a discontinuity in March, 2001 and a reduction rate of 1.18615 million km^2/10yr and 294.600 thousand km^2/10yr for the two periods, respectively. However, from March, 2001 to December, 2015, there was a larger growth at a rate of 1.19856 million km^2/10yr.

5 Conclusions

Based on the TRMM precipitation data, the Precipitation Abnormity Percentage drought model was used to study the spatial distribution and spatio-temporal variation patterns of drought from 1998 to 2015 in the N50° area along the Belt and Road region. The area was divided into six sub-regions based on the economic corridors and the BFAST tool was used to analyze the regional drought characteristics in the research area. Overall, our study on drought distribution and its analysis in the Belt and Road area can be concluded as follows:

(1) Spatio-temporal analysis indicates that drought in this region showed obvious seasonal periodicity. In winter, the drought was mainly distributed in Northeast Asia, Southeast Asia, and South Asia, but in summer the drought was mainly distributed in Central Asia and West Asia. The drought area in winter was larger than in summer. As the season changes from spring to winter, drought areas continue to move west and during winter, severe drought returned to the eastern part of Asia. According to the statistical analysis, it was found that the drought area in the Belt and Road area reached a maximum of 23.2529 million km^2 in December, 1999 while the area of extreme drought accounted for 42.43% of the total drought area, and the drought reached a minimum of 7.8867 million km^2 in May, 2010 while the severe drought area accounted for 23.35% of the total drought area. The total area of drought in the Belt and Road region between 1998 and 2015 decreased at a rate of 40,260 km^2 per year, mainly in Northeast Asia, South Asia, and West Asia and North Africa.

(2) Through the spatio-temporal analysis of each sub-region, it was found that the occurrence and distribution of drought had obvious regional differentiation patterns. The average drought conditions in Northeast Asia, Central Asia, and West Asia were at the moderately dry level and below and the average drought condition in Southeast Asia and Central and Eastern Europe were mildly dry and no drought. The drought in South Asia was more severe and mostly in the severely dry and moderately dry levels. From 1998 to 2015, the average drought conditions in Northeast Asia, West Asia and North Africa, South Asia, and Central and Eastern Europe showed a decreasing trend over a small range. The growth rates of Precipitation Abnormity Percentages were 0.012/10yr, 0.072/10yr, 0.036/10yr, and 0.024/10yr, respectively. The change of average drought condition in Central Asia showed an increasing trend over a small range and the rate of reduction of Precipitation Abnormity Percentage was 0.036/10yr. The average drought condition in Southeast Asia showed a fluctuating pattern of first decreasing and then increasing, wherein from January, 1998 to August, 2002 the drought level decreased and the increment rate of the Precipitation Abnormity Percentage was 1.5/10yr. From September, 2002 to December, 2015, the drought level showed an increasing trend but in June, 2005 and June, 2010, there were two break points. The rates of decrease of the Precipitation Abnormity Percentage during the three time periods were 0.384/10yr, 0.24/10yr, and 0.552/10yr, respectively.

In this study, TRMM precipitation data were used to describe the occurrence and trends of drought, which are valuable for revealing the spatio-temporal distribution characteristics of droughts in the Belt and Road area. From the point of view of agricultural production, it is expected that further studies will take into consideration geographical factors such as soil water status, soil type, slope, crop drought tolerance, and agricultural production data and further study the direct impacts of drought on agricultural production.

References

Huete A R. 1988. A soil-adjusted vegetation index (SAVI). *Remote Sensing of Environment*, 25 (3): 295–309.

Big Data Center for the Belt and Road Initiative in National Information Center. 2016. Big data report of the Belt and Road Initiative (2016)[M]. Beijing, the Commercial Press. (in Chinese)

Chen J, Shi P, Wang D X, *et al*. 2007. Spatial distribution and seasonal variability of the rainfall observed from TRMM Precipitation Radar (PR) in the South China Sea Area (SCSA). *Advances in Earth Science*, 20 (1): 29–35. (in Chinese)

China Meteorological Administration. GB/T20481-2006. Classification of Meteorological Drought[S]. (in Chinese)

China News Service. 2015. United Nations: Annual global losses from natural disasters as much as $300 billion[OL]. http://www.chinanews.com/gj/2015/03-05/7104479.shtml. (in Chinese)

Wilhite D A. 2000. Drought as a natural hazard: Concepts and definitions. *Drought A Global Assessment*, 1: 3–18.

Han L Y, Zhang Q, Yao Y B, *et al*. 2014. Characteristics and origins of drought disasters in Southwest China in nearly 60 years. *Acta Geographical Sinica*, 69 (5): 632–639. (in Chinese)

Bartholic J F, Namkem L N, Wiegand C L. 1962. Aerial Thermal Scanner to Determine Temperatures of Soils and of Crop Canopies Differing in Water Stress. *Agronomy Journal*, 64 (5): 603–608.

Quan J L, Zhan W F, Chen Y H, *et al*. 2016. Time series decomposition of remotely sensed land surface temperature and investigation of trends and seasonal variations in surface urban heat islands. *Journal of Geophysical Research Atmospheres*, 121: n/a-n/a.

Verbesselt J, Hyndman R, Newnham G, *et al*. 2010. Detecting trend and seasonal changes in satellite image time series. *Remote Sensing of Environment*, 114(1): 106–115.

Verbesselt J, Zeileis A, Herold M. Near real-time disturbance detection using satellite image time series. *Remote Sensing of Environment*, 2012, 123(123): 98–108.

Rouse J W, Haas R W, Schell J A, *et al*. 1974. Monitoring the vernal advancement and retrogradation (Greenwave effect) of natural vegetation. NASA/GSFCT Type III final report. Nasa.

Li J G, Ruan H X, Li J R, *et al*. 2010. Application of TRMM precipitation data in meteorological drought monitoring. *Journal of China Hydrology*, 30 (4): 43–46. (in Chinese)

Liu G S, Guo A H, An S Q, *et al*. 2004. Research progress in Palmer drought severity index and it's application. *Journal of natural disasters*, 13 (4): 21–27. (in Chinese)

Liu H, Liu R G, Liu S Y. 2012. Review of drought monitoring by remote sensing. *Journal of Geo-information Science*, 14 (2): 232–239. (in Chinese)

Ma H T. 2006. Exploring on correction and error sources of remote sensing image: taking Jixi city as an example[C]. Annual meeting of China land society. (in Chinese)

National Development and Reform Commission, Ministry of Foreign Affairs, and Ministry of Commerce of the People's Republic of China. 2015. Vision and Actions on Jointly Building Silk Road Economic Belt and 21st-Century Maritime Silk Road. *Finance & Accounting for Communications* (4): 82–87. (in Chinese)

Pei H J. 2016. Global natural disasters in 2015 dominated by meteorological disasters. Monitoring express of resources and environmental science development (5): 11–12. (in Chinese)

Curran P J. 1979. The use of polarized panchromatic and false-color infrared film in the monitoring of soil surface moisture. *Remote Sensing of Environment*, 8 (3): 249–266.

Qi S H, Zhang Y P, Niu Z, *et al*. 2005. Application of water deficit index in drought monitoring in China with remote sensing. *Acta Pedological Sinica*, 42 (3): 367–372. (in Chinese)

Ren S Y. 1991. Research on drought concept. *Agricultural Research in the Arid Areas*, 1: 78–80. (in Chinese)

Sun Z H, Wang Z L, Cao X M, *et al*. 2014. Application of 3 drought evaluation indices of the Loess Plateau in Shaanxi Province. *Chinese Agricultural Science Bulletin*, 30(20): 308–315. (in Chinese)

UNISDR, CRED. 2016. 2015 disasters in numbers. UNISDR PUBLICATIONS.

Wang Y W. 2015. Challenges and opportunities of the Belt and Road Initiative [M]. Beijing, People's Publishing House. (in Chinese)

Che X H, Yang Y P, Feng M, *et al*. 2017. Mapping Extent Dynamics of Small Lakes Using Downscaling MODIS Surface Reflectance. Remote Sensing, 9 (1): 82-103.

Xiao Z S. 2016. Numbers in the Belt and Road area[M]. Beijing, Commercial Press. (in Chinese)

Ye D Z. 1996. Study on regularity and cause of flood and drought in the Yangtze River and the Yellow River Basin[M]. Shandong, Shandong science and technology press. (in Chinese)

Zhang J S. 1993. Definition of drought and its logical analysis. *Agricultural Research in the Arid Areas*, (3): 97–100. (in Chinese).

基于 TRMM 降水数据的 1998–2015 年“一带一路”干旱时空分布

柏永青[1,2]，王卷乐[1,3]，王玉洁[1,4]，韩雪华[1,2]，Bair Z. Tsydypov[5]，Altansukh Ochir[6]，Davaadorj Davaasuren[7]

1. 中国科学院地理科学与资源研究所 资源与环境信息系统国家重点实验室，北京 100101；
2. 中国科学院大学，北京 100049；
3. 江苏省地理信息资源开发与利用协同创新中心，南京 210023；
4. 山东理工大学，山东 淄博 255012；
5. 俄罗斯科学院西伯利亚分院贝加尔湖自然管理研究所，乌兰乌德 670047，俄罗斯；
6. 蒙古国立大学工程与应用科学学院，乌兰巴托 210646，蒙古；
7. 蒙古国立大学艺术和科学学院地理学系，乌兰巴托 210646，蒙古

摘　要：干旱是一种世界范围的自然灾害，长期影响各国农业生产和社会经济活动。“一带一路”沿线区域生态环境脆弱、农业耕地集中、干旱灾害频繁，利用遥感卫星监测大区域的干旱水平及其时空变化，对于科学掌握“一带一路”地区的干旱格局、区域分异特征，及其对农业耕地的影响具有重要的科学和现实意义。本文基于 TRMM 降水数据，利用降水距平百分率干旱模型研究和获取了 N50°以南的“一带一路”沿线地区 1998–2015 年逐月干旱时空分布，得知冬季的干旱主要分布在东北亚、东南亚和南亚地区，夏季的干旱主要分布在中亚和西亚地区，干旱的发生具有明显的季节周期性。利用 BFAST 算法以经济走廊为骨干划分六大片区分析了“一带一路”地区干旱的区域分异特征，可知 18 年来，东北亚、西亚北非、南亚和中东欧地区的干旱平均水平呈现小范围的减轻趋势，中亚地区的干旱平均水平呈现小范围的增强趋势，东南亚地区的干旱平均水平变化呈现先减后增的波动特征。1998–2015 年间“一带一路”地区的干旱总面积以每年 40260 km^2 的总趋势不断减少。

关键词：干旱时空分布；“一带一路”；TRMM；降水距平百分率；BFAST